

Article ID: 1007-4627(2017)03-0499-06

Cluster Radioactivity in Trans-lead Nuclei Reexamined

QIAN Yibin^{1,2}, REN Zhongzhou^{2,3}

(1. Department of Applied Physics, Nanjing University of Science and Technology, Nanjing 210094, China;

2. School of Physics, Nanjing University, Nanjing 210093, China;

3. School of Physics Science and Engineering, Tongji University, Shanghai 200092, China)

Abstract: We revisit the cluster emission from trans-lead nuclei within the density dependent cluster model. According to the refined density distribution of daughter and cluster via the available experimental data on nuclear charge radii and neutron skin thickness, the crucial cluster-core potential is constructed by the double-folding model. Then the Schrödinger equation of the cluster-core relative motion is solved along the outgoing Coulomb wave function boundary condition to obtain the decay width. The present decay width of cluster radioactivity is clearly augmented as compared to our previous results without the specific concern of the density distribution of daughter and cluster. Moreover, the computed decay width reduces along with the increasingly depressed density in the cluster center.

Key words: cluster radioactivity; nuclear radius; neutron skin

CLC number: O571.3

Document code: A

DOI: 10.11804/NuclPhysRev.34.03.499

1 Introduction

Cluster radioactivity, as a rare decay mode of unstable heavy nuclei, was firstly predicted by Săndulescu, Poenaru and Greiner via the superasymmetric fission model in 1980^[1]. Not long after, Lu *et al.*^[2] particularly indicate that the carbon emission from ^{223,224}Ra is the most probable candidate for this new kind of decay channel. Impressively, this phenomenon, ¹⁴C emitting from ²²³Ra, was really and truly confirmed in the experiment proposed by Rose and Jones four years later^[3]. From then on, extensive efforts have been devoted to this attractive subject in laboratories all over the world^[4-6]. Up to now, more than 20 cluster emissions (from ¹⁴C to ³⁴Si) mostly from various actinide isotopes, decaying to the doubly magic nucleus ²⁰⁸Pb or its neighboring nuclei, have been documented and reported through persistent search for such a peculiar and rare decay mode. Strikingly, the concept of cluster emission was recently enlarged to allow emission of quite heavier clusters ($Z > 28$) from superheavy isotopes aiming at daughter around ²⁰⁸Pb^[7, 8], which implies another possible decay choice of superheavy nuclei and somewhat stimulates the renewed interest in cluster radioactivity as

well.

As the intermediate case between alpha decay and nuclear fission, the spontaneously emitted particle in cluster emission is heavier than alpha particle but lighter than the lightest product in fission process. Consequently, it appears to be straightforward and convenient to treat the cluster radioactivity based on the alpha-like method^[9-13, 17-19] or the fission-like method^[1, 7, 8, 14-16]. As for the traditional alpha decay approach, the cluster is recognized to be preformed at the surface of parent nucleus before its penetration through the potential barrier. The cluster-preformation factor P_c , indicating the formation probability of emitted cluster, can be estimated by either some simple effective assumptions^[13, 14] or solving the Schrödinger equation of the dynamic flow of mass and charge^[11, 12]. With the help of the reasonable expression of the cluster preformation factor, several studies in the effective cluster model have been performed to satisfactorily give half-lives of cluster decay^[13, 14]. Besides, other related calculations have been improved by introducing the influence of nuclear deformations and orientations^[12]. Regarding to the fissionlike picture, the cluster decay process is treated as a consecutive evolution of geometrical shapes and the formation of

Received date: 18 Nov. 2016; **Revised date:** 22 Mar. 2017

Foundation item: Natural Science Foundation of China(11375086, 11535004, 11605089, 11120101005); Natural Science Youth Fund of Jiangsu Province (BK20150762); Fundamental Research Funds for the Central Universities (30916011339)

Biography: QIAN Yibin(1989-), male, Tianchang, Anhui, Lecturer, working on theoretical nuclear physics;
E-mail: qyibin@njust.edu.cn.

cluster is located at the adiabatic rearrangement of parent nucleus. Among these studies, the generalized liquid drop model has been early established to describe cluster emission, involving the macroscopic deformation energy surface plus the microscopic correction^[17]. Recently, the Thomas-Fermi approach is extended to construct a multidimensional model of cluster radioactivity via the introduction of shell ingredient with Skyrme and Coulomb forces^[18].

In fact, whatever the employed approach is, the penetration and preformation probabilities of the emitted cluster sensitively depend on the type of interaction potentials between cluster and residual. In this sense, the appropriate knowledge and the accurate components of the potential barrier are of great importance for the full understanding of this fascinating radioactive mode. Recently, we have improved the calculation on alpha decay half-lives by separately considering the proton and neutron density distribution in the density-dependent cluster model^[20–22], which was successfully employed into the description of cluster decay. Consequently, it is quite desirable to recognize the effect of the density distribution of the cluster-core system on cluster emission. Moreover, a few emitted clusters are exactly supposed to be candidates of bubble nuclei^[23, 24]. Whether the central-depressed density distribution of clusters brings corresponding modifications on the final result is a quite interesting problem and would be investigated presently. Meanwhile, the daughter nuclei are all around the typical nucleus ^{208}Pb , which possess available experimental data on neutron skin thickness in addition to plenty of data on nuclear charge radii^[25–27]. This provides us an excellent opportunity to deduce the convinced density distribution of related nuclei. In the next section, a brief introduction of theoretical approach, especially including the density distributions of daughter and cluster, would be given carefully. The detailed results and corresponding comparison are presented in Sec. 3, and the bubble effect of cluster on the decay process is discussed to some extent as well. Sequential conclusions are given in the last section.

2 Theoretical approach

2.1 Cluster-daughter system in the density-dependent cluster model

Given that the parent nucleus is a two-body system of the cluster interacting with the daughter nucleus, the interaction potential between them is believed to be the fundamental and crucial input for the half-life calculation of cluster emission. At present, their Coulomb potential is obtained by the double-

folding integral of the proton density distributions of clusters and daughters and standard proton-proton Coulomb interaction, while the nuclear part is consistently constructed by the same procedure but with the mass density distribution and the effective nucleon-nucleon (NN) interaction^[22]

$$V_N(\mathbf{r}) = \int d\mathbf{r}_1 d\mathbf{r}_2 (\rho_1^n(\mathbf{r}_1) + \rho_1^p(\mathbf{r}_1))(\rho_2^n(\mathbf{r}_2) + \rho_2^p(\mathbf{r}_2)) v(\mathbf{s} = |\mathbf{r}_2 + \mathbf{r} - \mathbf{r}_1|). \quad (1)$$

The density distributions of the daughter nucleus (ρ_1) and the cluster (ρ_2) are depicted via the widely used two-parameter Fermi (2pF) form,

$$\rho_{1,2}^\xi(r_{1,2}) = \frac{\rho_0^\xi}{1 + \exp\left(\frac{r_{1,2} - R_{1/2}^\xi}{a^\xi}\right)}, \quad (2)$$

where ξ is p or n, and ρ_0 is determined by integrating the density distribution equivalent to proton or neutron number of the corresponding nucleus. The half-density radius $R_{1/2}$ is related to the mass number of the cluster and the daughter, $R_{1/2} = cA^{1/3}$. The root-mean-square (rms) proton and neutron radii of the cluster or the daughter can then be obtained by

$$R^\xi \equiv \sqrt{\langle r^2 \rangle} = \left[\frac{\int \rho(r) r^4 dr}{\int \rho(r) r^2 dr} \right]^{1/2}. \quad (3)$$

As far as the nuclear potential is concerned, the effective NN interaction $v(\mathbf{s})$ is taken as the popular M3Y-Reid-type, and the details on the parameterized formulas and the specific computation can be found in Refs. [28, 29]. Once the nuclear and Coulomb potentials are built via the above process, the radial Schrödinger equation

$$\left(-\frac{\hbar^2}{2\mu} \frac{d^2}{dr^2} + V(r) \right) \varphi_{n\ell j}(r) = Q \varphi_{n\ell j}(r), \quad (4)$$

aiming at the cluster-daughter relative motion, would be solved to proceed the procedure. Here the total interaction potential $V(r)$ is composed of the attractive nuclear term, the repulsive Coulomb term, and the centrifugal part,

$$V(r) = \lambda V_N(r) + V_C(r) + \frac{\ell(\ell+1)\hbar^2}{2\mu r^2}, \quad (5)$$

where μ is the reduced mass of the cluster-core system measured in the unit of the nucleon mass $\mu = \frac{A_c A_d}{A_c + A_d}$, and ℓ is the angular momentum carried by the emitted cluster. The renormalization factor λ of nuclear potential is settled to adjust the experimental Q value and the number of internal nodes n in the radial wave function. This quantum number n is chosen according to the Wildermuth and Tang condition to satisfy

the main effect of the Pauli principle^[30]. It should be noted that the quantum number of cluster is connected with the shell-model quantum number of these nucleons forming the cluster in this way. Consequently, the quasibound solution $\varphi_{n\ell_j}(r)$ is obtained with the outgoing Coulomb wave function boundary condition^[31],

$$\varphi_{n\ell_j}(r) = N_{\ell_j}[G_\ell(kr) + iF_\ell(kr)], \quad (6)$$

where N_{ℓ_j} is the normalization constant, G_ℓ and F_ℓ are respectively the irregular and regular Coulomb wave functions with the wave number $k = \sqrt{2\mu Q}/\hbar$. Through a certain algebra and deduction, one can then obtain the decay width

$$\Gamma = \frac{\hbar^2 k}{\mu} |N_{\ell_j}|^2 = \frac{\hbar^2 k}{\mu} \frac{|\varphi_{n\ell_j}(R)|^2}{G_\ell(kR)^2 + F_\ell(kR)^2}, \quad (7)$$

which yields almost the same value regardless of the choice of R as long as its position is located beyond the nuclear potential. It is then indispensable to include cluster preformation factor P_c , measuring the extent to which the cluster is formed at the surface of parent nucleus, to achieve the absolute half-life of cluster decay. In turn, the P_c value can be extracted by dividing the experimental decay width by the calculated one $P_c = \Gamma_{\text{expt}}/\Gamma_{\text{calc}}$, where the experimental decay width is related to the experimental half-life via the well-known relationship $\Gamma_{\text{expt}} = \hbar \ln 2/T_{1/2}$ (measured data taken from Ref. [32]). In the meantime, the present pursuit of focusing on the effect of different proton and neutron density distributions of involved nuclei can be directly reached through this quantity. On the other side, the formation of clusters should decrease considerably in magnitude with the increasing of emitted cluster based on some available experimental facts. Moreover, provided that a given cluster can emit from different parent nuclei, the cluster preformation factor should correlate with the size of the parent or daughter nucleus. Keeping these in mind, the cluster preformation factor is populated to behave as^[14]

$$\log_{10} P_c = a\sqrt{\mu}(Z_c Z_d)^{1/2} + b, \quad (8)$$

where Z_c and Z_d are separately the atomic numbers of the cluster and the daughter. In this study, whether the extracted P_c values follow such a linear relationship is of great interest to be checked in detail, which is also quite valuable for the extension to unknown cluster emitters such as superheavy nuclei and lighter nuclei beyond the tin region.

2.2 Parameters in the density distribution of related nuclei

Before performing the detailed calculation, specific parameters in the 2pF formula of density distribution should be paid special attention to, which exactly

demonstrates the influence of density distribution of daughter and cluster on cluster emission. Previously, these parameters are usually fixed as the constants $R_{1/2} = 1.07A^{1/3}$ fm and $a = 0.54$ fm. However, it appears to be more reasonable and convincing to obtain them from experimental nuclear radii, while the crucial cluster-core potential is quite sensitive to their density distributions. Meanwhile, the phenomenon of neutron skin is considerable for heavy nuclei especially these daughter nuclei of cluster radioactivity, somewhat resulting in that the proton and neutron density distributions of daughter should be distinguished to probe into their effects on cluster emission. Fortunately, there have accumulated a great deal of experimental data on nuclear charge radii. Besides, although measurement on rms neutron radii or neutron skin thickness is quite limited as compared to the situation of nuclear charge radii, an effective relationship between the neutron skin thickness $\Delta R_{\text{np}} = R_n - R_p$ and the neutron-proton asymmetry term $I = (N - Z)/A$ is proposed as $\Delta R_{\text{np}} = (0.90 \pm 0.15)I + (-0.03 \pm 0.02)$ fm on the basis of available experimental data from coherent pion photo-production cross sections^[26]. It should be noted that this relationship is consistent with other theoretical calculations in the density function theory, and populates the $\Delta R_{\text{np}} = 0.160(52)$ fm for ^{208}Pb , being quite compatible with experiments^[27]. Here we adopt this simple and reliable formula to evaluate the neutron skin thickness of heavy daughter nuclei in cluster decay.

Despite the same 2pF formula of proton and neutron density distribution in daughter nuclei, they exhibit different parameters (c_1^p, a_1^p) and (c_1^n, a_1^n) . Obviously, their differences are just rooted from the neutron skin thickness, and there are two extreme cases figuring this discrepancy, namely the “neutron skin” type with $c^n > c^p$ and $a^n = a^p$ and the “neutron halo” type with $c^n = c^p$ and $a^n > a^p$. In detail, the diffuseness parameters of proton and neutron density distributions in daughter nuclei are fixed as the same value $a^p = a^n = 0.54$ fm for the “neutron skin” case, while the radius parameters c^p and c^n are separately determined from the rms proton and neutron radii. When it comes to the “halo” case, the diffuseness of proton density distribution in daughter is still fixed at $a^p = 0.54$ fm as usual but with the deduced c^p from the experimental charge radii. Then the parameter a^n can be obtained according to the rms neutron radius, $R_n = R_p + \Delta R_{\text{np}}$, accompanied by the same radius parameter $c^n = c^p$. In the contrast, the situation in normal light nuclei, *i.e.*, these emitted clusters, appears to be simpler due to the slight deviation between proton and neutron numbers. Hence the proton and neutron density distributions in clusters are assumed to behave in the same

way here. However, several light clusters are believed to act as candidates of bubble nuclei along with exotic density distributions^[23, 24]. In the present work, a three-parameter Fermi (3pF) formula is employed to further describe the density distribution of cluster

$$\rho_2(r_2) = \frac{\rho_0 \left(1 + \frac{\omega r_2^2}{R_{1/2}^2}\right)}{1 + \exp\left(\frac{r_2 - R_{1/2}}{a}\right)}, \quad (9)$$

to detect the effect of central depression of density in cluster on cluster decay. Additionally, ω (positive) affects the central density, and the depression degree increases with the increasing of ω value. For a deep insight, the depression degree, indicating the quantitative bubble effect, is defined to measure how the central density is depressed, $D = \frac{\rho_{\max} - \rho_{\text{cent}}}{\rho_{\max}} \times 100\%$, where ρ_{\max} and ρ_{cent} respectively present the maximum and central density value.

3 Numerical results and discussions

As mentioned before, the cluster-core potential is fundamental and pivotal for calculating the decay width of cluster emitters. In this sense, it is essential to check the change of the total potential versus different density distributions in daughter nuclei, leading to the final result. Here we take the decay $^{222}\text{Ra} \rightarrow ^{208}\text{Pb} + ^{14}\text{C}$ for example in Fig. 1, where the total interaction potential is plotted in three cases, namely the completely identical behavior of proton and neutron density distribution of daughter (or say $\Delta R_{\text{np}} = 0$), the aforementioned “neutron skin” type and “neutron halo” type daughter. Provided that the neutron skin means a more expanded neutron distribution, the potential well of the cluster-core system would be wider and the inner potential would be reduced as well. Indeed, one can see from this figure that the total potential with $\Delta R_{\text{np}} = 0$ is the deepest one in the interior region, but gradually ascends beyond others from the middle part of the routine and slightly locates above other lines in the penetration region before the coincidence of all potentials. In addition, the total potential of neutron halo case is located below that of skin case at the beginning of path similarly owing to the more extended neutron distribution in the former one, but they would behave in the same way then. Note that the barrier penetration probability of the cluster is extremely sensitive to the barrier beyond the decay energy Q . Combing these recognitions, one can conclude that the decay width in the case $\Delta R_{\text{np}} = 0$ should be clearly reduced as compared to that in either halo or skin case of daughter, and the

results in the two latter cases are quite close to each other.

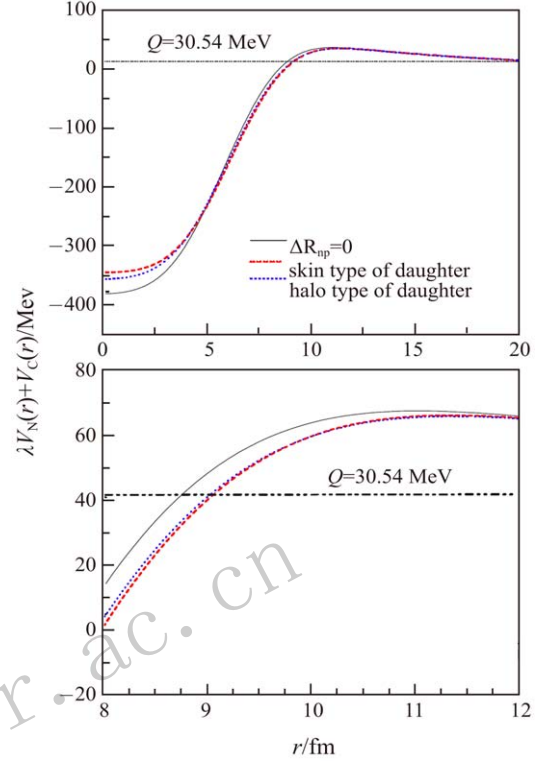


Fig. 1 (color online) Schematic sketch of the total potential $V(r) = \lambda V_N(r) + V_C(r)$ between daughter and cluster for the cluster emission $^{222}\text{Ra} \rightarrow ^{208}\text{Pb} + ^{14}\text{C}$. The black line denotes the case without considering the neutron skin thickness, the red dashed line presents the neutron skin type distribution with $\Delta R_{\text{np}} = 0.160$ fm, and the blue dotted line gives the halo type case. To guide the eye, the magnified version of the potential in the range of $r = 8 \sim 12$ fm is plotted in the lower panel.

Next, the detailed results are demonstrated in Fig. 2, in order to check the above conclusion and give a better insight directly. Besides, this figure is plotted as the variety of extracted $P_c = \Gamma_{\text{expt}}/\Gamma_{\text{calc}}$ with the quantity $\sqrt{\mu}(Z_c Z_d)^{1/2}$, which can straight reveal the calculated value from different choices of density distribution and verify the trend as Eq. (8). As expected, the calculated decay width in the case without consideration of neutron skin thickness, is obviously smaller than other cases, no matter even-even nuclei or odd- A nuclei are concerned. In the meantime, the data points of skin type and halo type daughters generally coincide. Moreover, the relationship between these two quantities in Fig. 2 follow a linear line approximately, while the cluster preformation factor of even-even nuclei appears to be larger in contrast with that of odd- A nuclei for one given cluster because of the hindrance effect from unpaired nucleon.

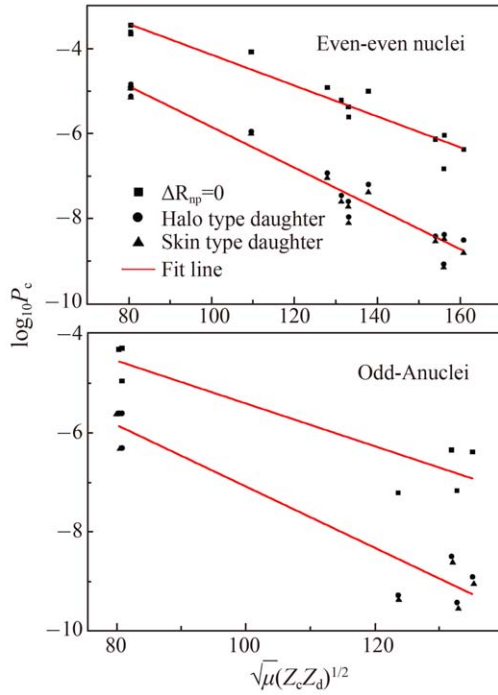


Fig. 2 (color online) Variation of extracted P_c value with the quantity $\sqrt{\mu}(Z_c Z_d)^{1/2}$ including the results in the three concerned cases and the correspondingly fitted line.

In the end, the role of the bubble clusters would be paid special attention to for the calculation of decay width in cluster radioactivity. As recommended in Ref. [23], $^{20,22}\text{O}$ are the probable candidates for the bubble nuclei, which hold quite clear depressed density in the central region. As mentioned before, the 3pF formula has been employed to depict the charge density distribution and the subsequential charge form factors of light nuclei^[24]. We make use of the 3pF density distribution of ^{20}O , as an example, to investigate the effect of the central depression on the final decay width of cluster emitters. Among this procedure, the half-density radius parameter $R_{1/2} = cA^{1/3}$ is determined by matching the constant nuclear radii for one ω , while the diffuseness a is settled as 0.46 fm to maintain the positive $R_{1/2}$ value and the positive depression in the center of cluster density. The larger the ω is, the more depressed the central density is corresponding to the larger D value. It is found that the calculated half-life ($P_c = 1$) increases with the raised ω value at the beginning, but the increasing trend slows down gradually, as can be seen in Fig. 3. Besides, the corresponding central depressed degree D is illustrated in the lower panel of the figure. When the depression D achieves approximately the theoretical value of 20% in Ref. [23], the calculated half-life would increase about 10% as compared with that without the deliberation of the central depression.

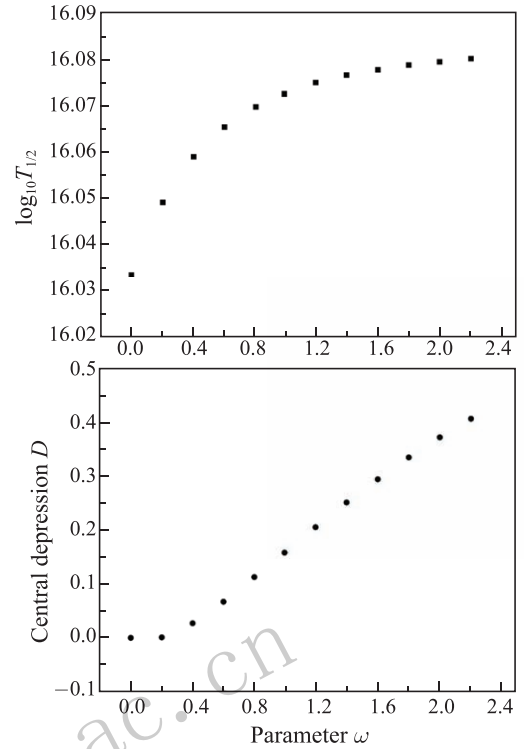


Fig. 3 Calculated half-lives with $P_c = 1$ versus the increasing of the depression parameter ω for the cluster emission $^{228}\text{Th} \rightarrow ^{208}\text{Pb} + ^{20}\text{O}$, which is located at the upper part. Correspondingly, the central depressed degree, defined as $\frac{\rho_{\max} - \rho_{\text{cent}}}{\rho_{\max}} \times 100\%$, is plotted in the lower part to present a comparable view.

4 Conclusions

By considering the specific proton and neutron density distributions from the combination of the experimental nuclear charge radii and the thickness of neutron skin, the crucial cluster-core potential in cluster radioactivity is carefully refined via the double-folding procedure. The decay width is then obtained within the density-dependent cluster model, and the calculated decay width of cluster emitter is largely enhanced once the density distribution of daughter nuclei is determined in above way. In other words, the preformation of one emitted cluster before its penetration appears to be more difficult in contrast with our previous thought. During the whole computation, two extreme types of daughter distribution, *i.e.*, neutron skin and neutron halo cases, are taken into account, and the decay widths in these two cases are quite close to each other. Furthermore, the calculated decay width of cluster emission is found to decrease with the increasing of the central depression in the cluster density.

References:

- [1] SĂNDULESCU A, POENARU D N, GREINER W. *Sov J Part Nucl*, 1980, **11**: 528.
- [2] LU X T, JIANG D X, YE Y L. *Nuclear Physics [M]*. Beijing: Atomic Energy Press, 2000: 127. (in Chinese)
(卢希庭, 江东兴, 叶沿林. *原子核物理[M]*. 北京: 原子能出版社, 2000: 127.)
- [3] ROSE H J, JONES G A. *Nature (London)*, 1984, **307**: 245.
- [4] BONETTI R, GUGLIELMETTI A. *Romanian Rep Phys*, 2007, **59**: 301.
- [5] GUGLIELMETTI A, FACCIO D, BONETTI R, *et al.* *J Phys: Conf Ser*, 2008, **111**: 012050.
- [6] LOVAS R G, LIOTTA R J, INSOLIA A, *et al.* *Phys Rep*, 1998, **294**: 265.
- [7] POENARU D N, GHERGHESCU R A, GREINER W. *Phys Rev Lett*, 2011, **107**: 062503.
- [8] POENARU D N, GHERGHESCU R A, GREINER W. *Phys Rev C*, 2012, **85**: 034615.
- [9] BLENDOWSKE R, WALLISER H. *Phys Rev Lett*, 1988, **61**: 1930.
- [10] BUCK B, MERCHANT A C. *Phys Rev C*, 1989, **39**: 2097.
- [11] MALIK S S, GUPTA R K. *Phys Rev C*, 1989, **39**: 1992.
- [12] ARUN S K, GUPTA R K, SINGH B B, KANWAR S, SHARMA M K. *Phys Rev C*, 2009, **79**: 064616.
- [13] REN Z Z, XU C, WANG Z J. *Phys Rev C*, 2004, **70**: 034304.
- [14] NI D D, REN Z Z. *Phys Rev C*, 2010, **82**: 024311.
- [15] ZHANG H F, DONG J M, ROYER G, *et al.* *Phys Rev C*, 2009, **80**: 037307.
- [16] ZHANG G L, LE X Y. *Nucl Phys A*, 2010, **848**: 292.
- [17] ROYER G, GUPTA RAJ K, DENISOV V YU. *Nucl Phys A*, 1998, **632**: 275.
- [18] DENISOV V YU. *Phys Rev C*, 2013, **88**: 044608.
- [19] SANTHOSH K P, BIJU R K, SAHADEVAN S. *Nucl Phys A*, 2010, **838**: 38.
- [20] QIAN Y B, REN Z Z. *Phys Lett B*, 2014, **738**: 87.
- [21] NI D D, REN Z Z. *Phys Rev C*, 2015, **92**: 054322.
- [22] QIAN Y B, REN Z Z. *J Phys G: Nucl Part Phys*, 2016, **43**: 065102.
- [23] SHUKLA A, ÅBERG S, BAJPEYI A. *Phys At Nucl*, 2016, **79**: 11.
- [24] CHU Y Y, REN Z Z, WANG Z J, *et al.* *Phys Rev C*, 2010, **82**: 024320.
- [25] ANGELI I, MARINOVA K P. *At Data Nucl Data Tables*, 2013, **99**: 69.
- [26] WARDA M, VIÑAS X, ROCA-MAZA X, *et al.* *Phys Rev C*, 2010, **81**: 054309.
- [27] TARBERT C M, WATTS D P, GLAZIER D I, *et al.* *Phys Rev Lett*, 2014, **112**: 242502.
- [28] SATCHLER G R, LOVE W G. *Phys Rep*, 1979, **55**: 183.
- [29] KOBOS A M, BROWN B A, HODGSON P E, *et al.* *Nucl Phys A*, 1982, **384**: 65.
- [30] WILDERMUTH K, TANG Y C. *A Unified Theory of the Nucleus[M]*. New York: Academic Press, 1997.
- [31] LIOTTA R J. *J Phys: Conf Ser*, 2013, **413**: 012012.
- [32] AUDI G, KONDEV F G, WANG M, *et al.* *Chin Phys C* 2012, **36**: 1157.

铅以上核结团放射性再研究

钱以斌^{1,2,1)}, 任中洲^{2,3}

- (1. 南京理工大学应用物理系, 南京 210094;
2. 南京大学物理学院, 南京 210093;
3. 同济大学物理科学与工程学院, 上海 200092)

摘要: 在密度依赖的结团模型下重新研究了铅以上原子核的结团放射性。根据由核电荷半径以及中子皮厚度的实验数据所提炼的子核和结团密度分布, 通过双折叠模型得到了关键的结团-核芯作用势。然后结合库仑波函数边界条件求解了结团-子核相对运动的薛定谔方程, 以得到衰变宽度。和我们以往没有考虑子核和结团密度具体分布的计算结果相比, 现在得到的结团放射性衰变宽度明显增大。另外, 随着结团中心越来越高的密度压低, 衰变宽度的计算值会减小。

关键词: 结团放射性; 核半径; 中子皮

收稿日期: 2016-11-18; 修改日期: 2017-03-22

基金项目: 国家自然科学基金资助项目(11375086, 11535004, 11605089, 11120101005); 江苏省自然科学基金资助项目(BK20150762); 中央高校基本科研业务费(自主科研专项)(30916011339)

1) E-mail: qyibin@njust.edu.cn.